Climate Services 30 (2023) 100374

Contents lists available at ScienceDirect

Climate Services

journal homepage: www.elsevier.com/locate/cliser

# Copernicus global crop productivity indicators: An evaluation based on regionally reported yields

Sneha Chevuru [a,b,*], Allard de Wit [c], Iwan Supit [a], Ronald Hutjes [a]

[a] Department of Environmental Sciences, Water System and Global Change, Wageningen University and Research, The Netherlands
[b] Department of Physical Geography, Faculty of Geosciences, Utrecht University, The Netherlands
[c] Wageningen Environmental Research, Earth Observation, and Environmental Informatics, Wageningen University and Research, The Netherlands

ARTICLE INFO

*Keywords:*
Crop productivity
Climate change service
Skill

ABSTRACT

Climate variability places significant pressure on climate-sensitive sectors such as agriculture. Information on crop-related climate and water indicators under climate change becomes essential. The Copernicus Climate Change Service (C3S) provides reliable information about climate change based on climate models, Earth Observations, and in situ data to support adaptation policies. Within this C3S context, the Global Agriculture Sectoral Information System (SIS) has developed a new product based on global crop productivity indicators to document the effects of climate variability on crop yield variability. This study focuses on the evaluation of climate-enhanced, earth observation (EO) based crop productivity indicators i.e., Total Weight Storage Organs (TWSO, equivalent to yield), Total Above Ground Production (TAGP). These variables provide insights into the Spatio-temporal variability of yield, productivity, and development of four major staple crops (rice, maize, soybean, and wheat) for their main production regions at the global scale for the period 2000–2018. In this study, the evaluation was carried out spatially and temporally for the United States of America, India, and China for the period 2000–2018, using reported yield statistics aggregated to the lowest available administrative level of each region. For almost all the crops in the three countries, the skilled error can be reduced by more than 25% for both the indicators TAGP and TWSO compared to the trend of reported yield, suggesting considerable performance in assessing interannual yield variability. Results indicated both indicators individually performed well in many important producing areas of the USA, India, and China. However, if we compare both the indicator's performance in terms of production totals in the USA, India, and China, TAGP contributes ~27–50% of total crop production in the USA and India, and ~47–75% in China. While, TWSO contributes ~24–41% in the USA and India, and 5–65% in China.

**Practical Implications**

Climate change variability puts significant pressure on sensitive climate-sensitive sectors such as agriculture and the food sector. Extreme variations of seasonal rainfall and a strong temperature increase together with rising demand for food set extra pressure on natural resources and food systems. Hence, it is important for farmers and agencies such as crop yield forecasting and monitoring agencies and commodity traders, to adapt their food production and trade strategies according to variations and long-term climate changes to ensure food security. To deal with these challenges, information on crop productivity as influenced by weather variability is required. This paper addresses how this information can be obtained from various data sources such as remote sensing information and crop models in combination with climate data. Additionally, this paper presents an evaluation as well. In Copernicus Climate Change Service (C3S), a product 'climate enhanced Earth Observed (EO) based crop productivity indicators' (further referred to as "AgDMP") has been developed that combines the Global Weather for Agriculture (AgERA5) daily weather information (derived from European Centre for Medium-Range Weather Forecasts Reanalysis v5 (ERA5)) with the satellite products from Copernicus Global Land Service (GLS) and together with crop models. These global products consist of satellite-constrained, simulated growth and development of major crops (wheat, maize, soybean, and rice) on a 10x10 km grid at dekad (i.

* Corresponding author.
*E-mail address:* s.chevuru@uu.nl (S. Chevuru).

https://doi.org/10.1016/j.cliser.2023.100374
Received 24 September 2021; Received in revised form 17 January 2023; Accepted 11 April 2023
Available online 24 April 2023
2405-8807/

e. 10-day) intervals. Because of the long heritage of both Copernicus satellite products and ERA5 and their continuous updates, the products provide both near real-time data as well as a consistent archive, dating back to 1999, which is valuable for identifying current anomalies against the long-term average.

The world's staple food commodities such as maize, soybean, rice, and wheat contribute approximately 64% of agriculture's calorie production. Variability in these crop production and quality, caused by weather conditions over its growing season is one of the reasons for crop price volatility. Production plants for major foodstuffs require a steady supply of these products to operate efficiently, which requires predicting the expected production for major production areas. Also, the efficiency of logistics can be improved when the availability of transport equipment is combined with insight into the expected spatial distribution of production. Such information is also relevant for optimizing sourcing strategies by the processing industry, allowing e.g., better choices between fixed contract or variable market buying schemes. Therefore, the AgDMP product provides crop yield information that can be used to place current conditions into a historical context.

Thus, this AgDMP data is highly relevant for many users in the agricultural community as well as for assessments of crop development and related anomalies of climate for the consecutive cropping season. However, this is particularly true for agro-business communities (such as commodity traders, cattle feed buyers, etc) and agro-policy makers. Early signs of production anomalies are of high importance for price volatility, tax/subsidies, logistics, and shortfall of production. Some of the potential users, for instance, are institutions for global crop monitoring and yield forecasting. Moreover, the AgDMP product is useful in various application domains such as for early warning purposes to detect the anomalies in crop growth, identify the zones of high or low productivity and be useful in agro-meteorological models to estimate and forecast the crop yield.

**Data availability**

I have shared the link to my data

## 1. Introduction

Climate change variability puts significant pressure on climate-sensitive sectors such as the agriculture sector. Extreme variations in seasonal rainfall and a strong increase in temperature together with rising demand for food set extra pressure on natural resources and food systems (Buontempo et al., 2019). Hence, farmers and agencies need to adapt their food production and trade strategies according to variations and long-term climate changes to ensure food security. For this purpose, information on crop-relevant climate and water indicators under climate change and climate variability become essential.

On a global scale, the Group on Earth Observation (GEO) provides information on global agriculture through its GEO Global Agricultural Monitoring (GEOGLAM) program (Becker-Reshef et al., 2018). GEOGLAM coordinates and integrates the efforts from operational crop monitoring systems globally which include earth observation products, crop modeling, and in-situ observations of agricultural production. The monthly bulletins generated by GEOGLAM feed into the Agricultural Market Information System (AMIS) to enhance food market transparency and policy response for food security (Becker-Reshef et al., 2019).

Copernicus, which is a spinoff of the European Union's Earth Observation Programme provides open-access data related to many earth components based on earth observation, in-situ measurements, and modeling. Among one of the services, the Copernicus Climate Change Service (C3S) provides a set of operational services with consistent and authentic, climate-derived information. Aimed at the agriculture and food sector, it also provides decision-makers/end users with pertinent, credible, and legitimate agro-climatic data products.

In recent years, Copernicus Global Land Service (CGLS) developed a bio-geophysical product to support users for global vegetation monitoring. One of the products, Dry Matter Productivity (DMP) [1] represents the growth rate of dry biomass. The product DMP (version 1) at 300 m resolution is derived from the sensor data of SPOT-VGT, PROBA-V, and currently Sentinel-3. The product calculates the DMP globally and makes it available near-real-time to the users, every 10 days. Therefore, in principle, these data are helpful to make day-to-day decisions on vegetation management, including crop monitoring and yield forecasting.

However, the current DMP product has several limitations for agricultural applications. First of all, the DMP product uses a Light Use Efficiency (LUE) approach for converting intercepted solar radiation into estimates of biomass growth rate. The LUE values used for DMP are representative of broad classes of vegetation types instead of crop-specific values which makes the product not consistent in estimating crop productivity. Second, the standard DMP product has no concept of cropping cycles which makes the product harder to interpret as it is not aligned with local cropping calendars. Moreover, the lack of cropping cycles also prohibits the implementation of a phenological model that would allow computing the harvestable product (e.g. the yield) from the total biomass. Finally, no crop masks have been implemented in the DMP product which means that users of DMP must still process the data spatially (where is the crop growing that I am interested in) and temporally (when is the crop on the field) which is complicating its use in crop monitoring systems.

Recently, C3S has completed a new product 'climate enhanced Earth Observed (EO) based crop productivity indicators' (AgDMP). This product is generated in a similar approach to DMP but with several improvements that make the product more suitable for agriculture (see next section). These AgDMP indicators provide insights into the Spatio-temporal variations of crop yield and productivity for major production regions globally. As an improved and operational product, the AgDMP product has the potential to enhance the capabilities for global agricultural monitoring and to become part of the suite of products that are used by GEOGLAM and other crop monitoring systems.

Providing relevant and credible data over long periods to the users and maintenance of operational forecasting activities requires a proper formal validation of the product results against ground truth, i.e., the reported/official yield and production statistics. Therefore, the objective of this study is to evaluate the AgDMP product for each of the four main crops (rice, maize, soybean, and wheat) in three major but contrasting production regions: the United States, China, and India. The simulated AgDMP indicators are generated over a period of 19 years, i.e. from 2000 to 2018, and we analyzed whether the simulated indicators could explain the interannual variability of crop yields at the regional level which is important for crop monitoring and yield forecasting systems.

## 2. Materials and methods

### 2.1. Detailed description of AgDMP product

The AgDMP product developed in the C3S provides insight into the yield and productivity of four major crops (rice, maize, soybean, and wheat) in their main global production regions from the period 2000- up till today. The algorithm developed for the AgDMP product represents a hybrid algorithm, that uses a satellite-derived Fraction of Absorbed Photosynthetic Active Radiation (FAPAR) with elements from the WOFOST (De Wit et al. 2019) and LINTUL (Adiele et al., 2021) crop

[1] https://land.copernicus.eu/global/sites/cgls.vito.be/files/products/CGLOPS1_SQE2017_TOCR1km-V1_I1.00.pdf.

simulation models. In this hybrid model, the simulation of the crop canopy is replaced by taking a satellite-derived FAPAR, computed from pixels with dominant cropping patterns for the four major crops. Similar to the LINTUL approach the net assimilation rate (kg dry matter ha-1 day-1) is calculated by multiplying the amount of intercepted light by a crop-specific light use efficiency (LUE) and temperature function for photosynthesis (RAR – Reduction Assimilation Rate). It applies the phenological model from WOFOST to determine the cropping season length in terms of growing degree days (GDD) about the thermal time requirements of the crop (TSUM). Finally, based on the crop's development stage (DVS) and crop-specific allocation parameters ($f_{ALL}$), a fraction of assimilates is allocated between stems, leaves, and grains.

Several static and dynamic input data sources were used in developing the more crop-relevant EO-based indicators. Fig. 1 shows the algorithm developed for the AgDMP product. The respective color boxes show the data products from different sources. The meteorological data at a 0.1-degree global resolution were taken from the ERA-INTERIM MARS archive up till 2018 while the agERA5 product is being used for generating the real-time AgDMP product (2019 up till today). The satellite-observed FAPAR data used are provided by the Copernicus Global Land Service at 1 km spatial resolution and at dekadal (10-daily) time steps. The static data includes crop calendars, crop masks, and crop parameters. Crop calendars used were collected from the Center for Sustainability and the Global Environment (SAGE) (Sacks et al. 2010) and the Global Agro-ecological Zonation (GAEZ), which are retrieved from the FAO website (https://www.fao.org/nr/gaez/en/). The crop dominance mask (*CDmsk*) was collected from Global Food Security Support Analysis Data (GFSAD). This enables us to create a 'pseudo' crop-specific mask for maize, wheat, soybean, and rice, allowing us to focus on areas with dominating cropping patterns. Crop parameters from the WOFOST and LINTUL crop parameter datasets (https://wageningenur.nl/wofost and https://models.pps.wur.nl/) are used.

The current version of the AgDMP product does not include a water balance and hence no water limitations on crop growth are taken into an account directly. However, we assume that water stress will be reflected in the satellite-observed FAPAR due to a reduction in leaf area because of drought stress, and thus severe drought stress on crop growth is taken into account indirectly.

The AgDMP product contains three variables (de Wit and Hutjes 2019):

1. Crop total weight storage organs (TWSO) in kg/ha, which represents the harvestable product (e.g. the yield);
2. Crop total above-ground biomass (TAGP) in kg/ha, which represents the sum of above-ground biomass components (stems, leaves, storage organs);
3. Crop Development Stage (DVS) which is a dimensionless indicator representing crop phenological development. DVS equals 0.0 at emergence, 1.0 at anthesis (flowering), and 2.0 at physiological maturity.

For details see the Algorithm Theoretical Basis Document[2].

#### 2.1.1. Data file contents and data structure

The AgDMP output variables are available in NetCDF files which represent the global coverage for a given crop, variable, time step, season ID, and campaign year (Fig. 2). A campaign year is defined as the calendar year when the harvest of the crop takes place. The total length of a campaign year can be more than a calendar year since cropping calendars differ from region to region. For instance, the campaign year of 2010 for soybeans, starts with the sowing of soybeans in Oct/Nov 2009 in Argentina which are harvested in 2010 June. Whereas, in Northern China, the sowing starts in April 2010 and the last soybeans of the 2010 campaign year are harvested in October while the campaign year for 2011 of soybeans in Argentina has already started. Having the campaign year definition allows distinguishing between those two campaigns.

Furthermore, rice can have two growing seasons in one campaign year, particularly in South- East Asia. Therefore, the data include a season id with values 1 or 2 for double rice cropping in a single campaign year. Also, winter and spring wheat are treated separately for one campaign year. Finally, the technical implementation of the output variables is such that their values are available in the NetCDF output up till the end of the campaign year. So although the crop is harvested and removed from the field, the simulated DVS, TWSO, and TAGP will remain in the NetCDF file up till 31 December of the campaign year (Fig. 3). This facilitates the aggregation of AgDMP results over areas with varying cropping calendars.

#### 2.1.2. Data for the study

The TWSO and TAGP indicators available at C3S[3] are used in this study. The four major crops (rice, maize, soybean, and wheat) are considered for the period 2000–2018. In some regions, rice crops can have two cropping seasons, hence the average of both is used for the study. Similarly, winter and spring wheat crops are combined in a regional average for wheat. The overview of the methodology is shown in Fig. 4.

#### 2.1.3. Extraction of NETCDF file data

The indicator data stored in NETCDF files have been visualized or examined by using ArcGIS software. The country-specific lowest administrative region levels mean data of four crops for the three countries the USA, China, and India were extracted and used for further processing.

### 2.2. Study area and reported statistics

The indicator data are generated globally for the four main crops (rice, maize, soybean, and wheat). This study focuses on the three countries with major production contributions to world food resources: the United States of America, China, and India. Furthermore, the usage of crop management and inputs for the three countries differs widely. Therefore, the evaluation not only covers climate variability but also crop management and inputs. Also, assuming that the reported crop yield statistics represent the true crop yield for all three countries. Since crop development is not systematically reported on any usable scale, the DVS indicator cannot be validated.

#### 2.2.1. United States of America (USA)

Major crops grown in the USA are maize and soybean followed by wheat and rice. Most of the maize and soybean are produced in the north-central region, also known as the 'corn belt'. Only a minor amount of production is grown in the southeast region.

The dominant cropping systems are continuous maize and alternating maize and soybean 2-year rotation. The central and eastern regions of the corn belt have favorable climate conditions for rainfed crops. Annual rainfall ranges from 800 to 1100 mm. The western region of the corn belt has less rainfall and includes the eastern great plains. Generally, soils are deep, fertile, rich in organic matter, and have a large water-holding capacity in rooting soil depth. Mollisols and Alfisols are the dominant soils (Connor et al. (2011) and Grassini et al. (2014)). In wet periods, water logging is a major problem in some central and eastern regions, where currently subsurface tile drainage is used to mitigate the problem on almost one-third of the total cropping land (Sugg, 2007).

[2] https://datastore.copernicus-climate.eu/documents/sis-global-agriculture/C3S422Lot1_WEnR_DS3b_AlgorithmTheoreticalBasis_Ver2.pdf.

[3] https://cds.climate.copernicus.eu/#!/home.

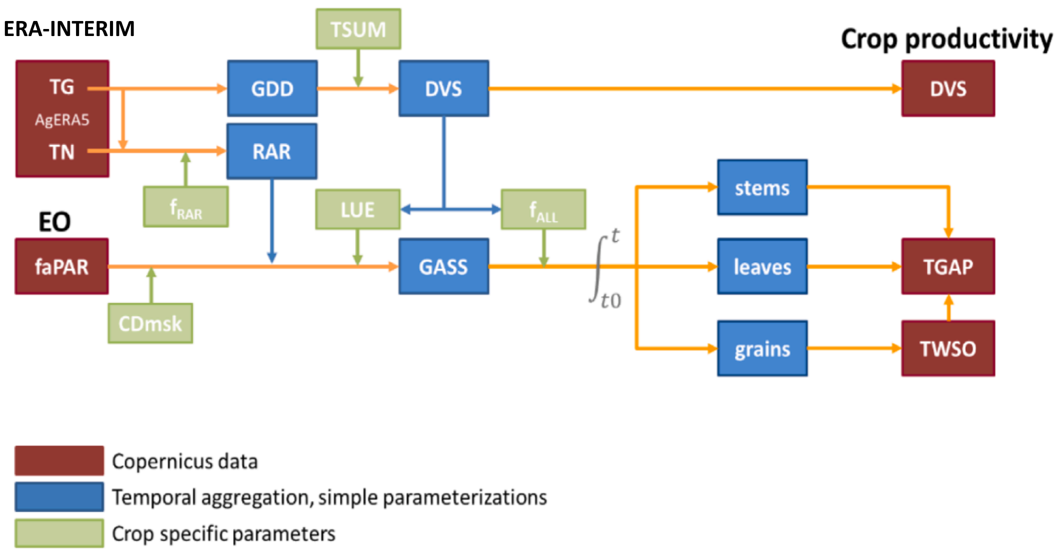


**Fig. 1.** Overview of the algorithm developed for the AgDMP product, see text for an explanation. https://climate.copernicus.eu/sites/default/files/2019-11/04%20Hutjes_ClimateEnhancedEOdata4agriculture_RH_C3S422.pdf.

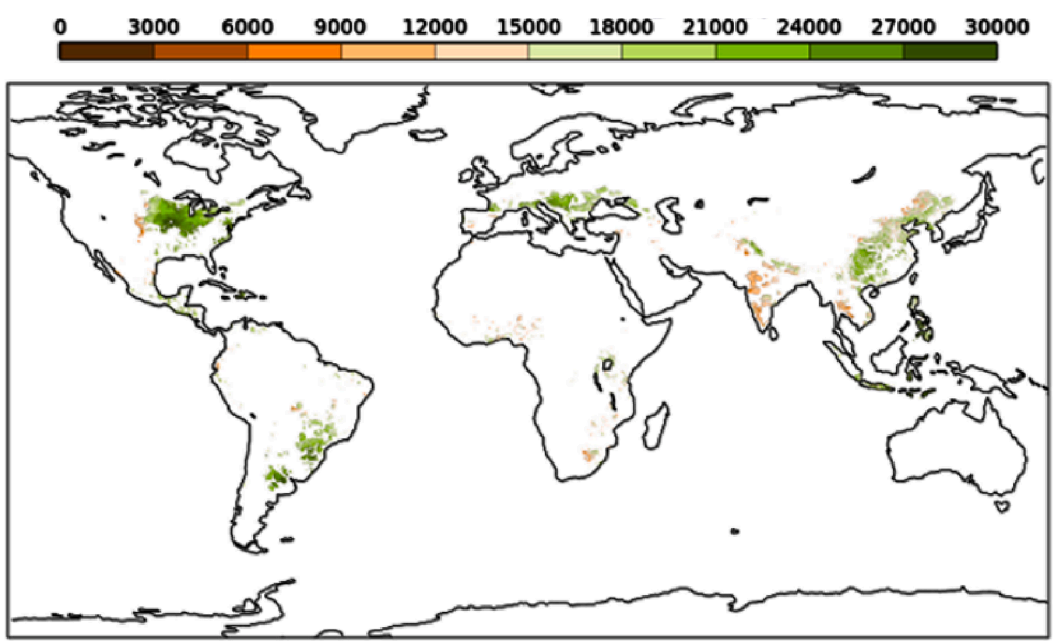


**Fig. 2.** Overview of the end-of-campaign total above-ground production (TAGP in kg/ha) for the year 2016 of Maize.

Rice production in the US has split into three ecological zones, the upper Sacramento Valley (California), the Gulf Coast (Texas, Louisiana, parts of Mississippi), and the Mississippi River Valley (Arkansas, Missouri, parts of Mississippi) (Livezey and Foreman, 2004).

The official reported census crop yields at the county level for all the states in the USA were collected from the United States Department of Agriculture (USDA) National Agricultural Statistics Service[4] for the period 2000–2018 for the crops rice, maize, soybean, and wheat. Not all states are useful for the study. For example, in Alaska, most crops are grown in a greenhouse and nursery.

### 2.2.2. China

Agriculture is one of the extremely important sources for China. Almost, 75% of the cultivated area in China is used for food crops (FAOSTAT,2014). The three major crops are rice, maize, and wheat. Human food occupies 80% of crop production, while 20% is allocated to animal feed (Kearney, 2010; Foley et al., 2011).

Generally, Indica and Japonica types of rice are sown in China. Indica-type rice occupies three-quarters of the area and Japonica the remaining. Japonica variety rice is mainly grown in the northern part and Indica in the southern parts. Within a year, two to three rice crops are grown in southern China, whereas a single rice crop is grown in northern China. Maize is mostly grown in north and northeast China. The wheat-growing regions in China are split into three agroecological zones: northern China's winter wheat region; southern China's winter and spring wheat regions. The northern winter wheat region is the

4 https://quickstats.nass.usda.gov/.

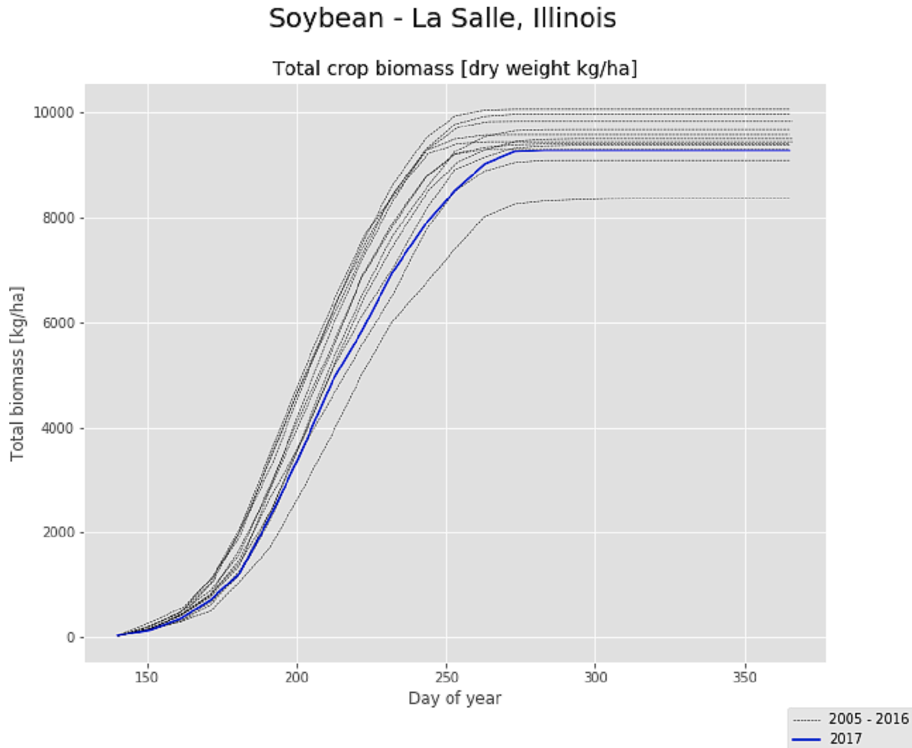


**Fig. 3.** Simulated total aboveground biomass (TAGP) for soybean for a La Salle county, Illinois. The blue line indicates a selected year (2017) while the grey lines represent different years over the period 2005–2016.

dominant production area for wheat.

The official reported crop yields of China were taken from the National Bureau of Statistics of China[5] yearbooks from 2000 to 2018 at the province level. Data for all 31 provinces were used in the study.

### 2.2.3. India

For half of the world's population, rice (Oryza sativa) is one of the staple foods (Muthayya et al., 2014). India alone produces 21% of the world's total rice production (Gadde et al., 2009). Among the total cropland area in India, rice and wheat occupy the largest share (Global Yield GAP Atlas). About cropping patterns, rice occupies a major cultivable area during the Kharif season (June to October). Wheat occupies the highest area during the Rabi season (November to March).

After rice and wheat, maize is India's second most popular crop. It is cultivated across all states in India. Majorly produced in north-central regions. Soybean is a minor production crop compared to rice, wheat, and maize. It is mainly grown as a summer crop in India (Krishisewa, 2013).

Official yield statistics at the district level were taken from the Economics and Statistics, Ministry of Agriculture[6] for the period of 2000–2018.

## 2.4. Analysis of reported yields and AgDMP time series

Fig. 5 shows the AgDMP indicator TWSO and the reported crop yield data of soybean in Illinois (USA) and maize in Inner Mongolia (China) from 2000 to 2019. For both regions, the reported yields show a clear trend over a period of twenty years. For instance, the reported average yield of soybean increased from 2.9 t/ha (average of 2000–2012) to 3.7 t/ha (average of 2013–2018) in Illinois. For Inner Mongolia, the maize yield increased from 5.4 tons/ha (average of 2000–2010) to 6.4 tons/ha (average of 2011–2018). This observed trend is mainly due to technological changes such as improved agricultural practices and crop varieties over this period (Arata et al., 2020). Further, an example of the TAGP indicator is shown in the supplementary in Fig. 15 and Fig. 16.

For the AgDMP indicator values represented by the TWSO variable, we did not expect such trends because the technology level is assumed stable. In other words, there is only a single set of parameters for the crop model that is used to generate the AgDMP product for the entire period 2000–2018. Nevertheless, in many of the regional aggregated data, we do find clear evidence of trends in the AgDMP data. For example, there is a clear trend in the TWSO for maize in Inner Mongolia. In contrast, no clear trend is visible in the TWSO values for soybean in Illinois (Fig. 5). Given that the crop model assumes a stable technology level, such trends in TWSO must be caused by systematic changes over time in the satellite-observed FAPAR data.

We hypothesize that this could be caused by two factors: 1) changes in the canopy due to increased inputs and 2) changes in the cropped area. The first factor is relevant in areas with relatively low yields, such as Inner Mongolia where crop yields are limited by inputs of fertilizer and/or disease control. Therefore increasing inputs over the period 2000–2019 (Smith and Siciliano 2015) lead to higher leaf area values and thus higher FAPAR values. In such environments, yield increases are driven by increases in the total light interception of the crop. In contrast, in areas with already high management inputs, such as Illinois, increases in crop yield are obtained through improved varieties (e.g. increasing harvest index) rather than increasing light interception because the crop canopy is already fully developed. On top of this, it is well known that satellite-derived variables such as NDVI, FAPAR, and LAI are less sensitive to dense canopies (Smith et al., 2020) and thus FAPAR values will not respond to changes in high input environments anyway.

The second factor that can explain the existence of systematic changes in FAPAR is a change in crop cultivated area. The crop mask that is used to select the relevant crop pixels from the GLS FAPAR product is derived from satellite observations from 2007 to 2012 (Thenkabail et al., 2010). Changes in the cropland area over time could

[5] https://www.stats.gov.cn/english/Statisticaldata/AnnualData/.
[6] https://eands.dacnet.nic.in/.

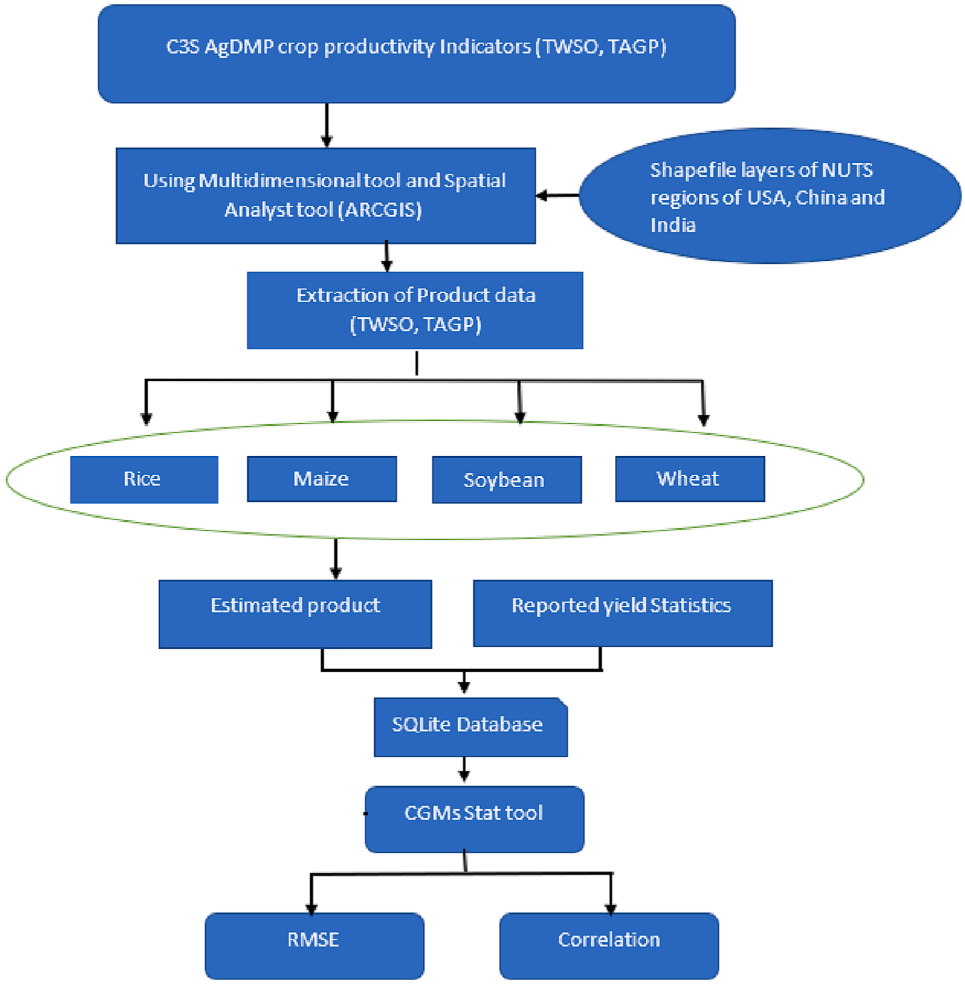


**Fig. 4.** Overview of the evaluation approach.

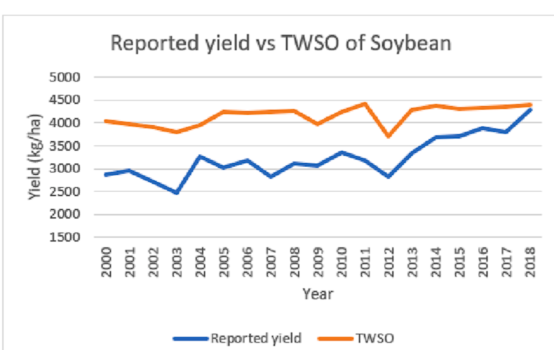


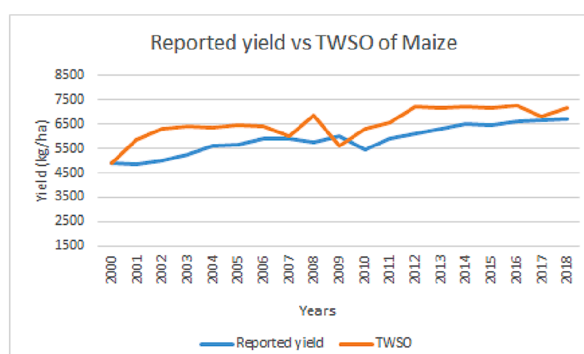


**Fig. 5.** Time series of reported crop yields and the AgDMP simulated value of TWSO for soybean in Illinois – USA (left) and Inner Mongolia – China (right).

have an impact on the average FAPAR values computed for the selected satellite pixels within a region. Nevertheless, we expect the impact on Inner Mongolia to be negligible given that Gao et al. (2019) report no significant change in cropland for this region in China.

*Statistical analysis and measures of skill*

The approach to analyzing the relationship between reported yield and AgDMP indicators is based on fitting a linear model to explain the time-series of reported yields of the form:

$$O_y = \overline{O} + b(y - \overline{y}) + c(P_y - \overline{P}) + \varepsilon_y$$

where $O_y$ is the reported yield $O$ for year $y$, $\overline{O}$ is the average reported yield, $b(y - \overline{y})$ is the technology trend where $b$ is the yearly increase/decrease in official yield, $c\ (P_y - \overline{P})$ is the modification of the trend by the AgDMP indicator $P$ (either TWSO or TAGP respectively) and regression coefficient $c$ and $\varepsilon_y$ is the residual error. In cases there is no trend in the reported yields, or where the trend in reported yield can be explained by a trend in the AgDMP indicator, the linear model reduces to:

$$O_y = \overline{O} + c(P_y - \overline{P}) + \varepsilon_y$$

The ability of the AgDMP indicators to explain the interannual variability in the reported regional crop yields can now be easily expressed by calculating the residual error in the regression model as a root mean squared error (RMSE).

However, without a reference, the RMSE itself is not a good measure of model skill. To interpret the RMSE from the regression model with the AgDMP indicators, it should be compared against the RMSE from a "naive" predictor, e.g. one that can be obtained without the use of AgDMP. In our study, this naive predictor (further to be called "baseline predictor") is provided by the RMSE of a linear trend model through the reported yields or, in case of no trend, by the RMSE of the average reported yield:

$$O_y = \overline{O} + b(y - \overline{y}) + \varepsilon_y$$

When the regression models that include the AgDMP indicators have "skill", it implies that the RMSE of those models is lower than the RMSE of the baseline predictor. In other words, the AgDMP product is only useful when it explains the interannual yield variability better than a simple trend model or average would do.

Next to the analysis based on the RMSE of the AgDMP indicator relative to the baseline predictor, we also computed the coefficient of determination ($R^2$) values between the reported yields and the predicted yields from the AgDMP indicators as an additional indicator that could be visualized.

Maps were generated that show spatial patterns in the RMSE of the models including the AgDMP indicators relative to the RMSE of the baseline predictor (the average or linear trend) expressed as a percentage reduction of RMSE. Similarly, correlation maps were constructed between the simulated indicators and reported statistics at 95 and 99% confidence intervals, color-coding it accordingly. Finally, the results were summarized and analyzed to understand the reasons behind the uncertainties and to examine where improvement is required.

The computations were done with the so-called "CGMS Statistical Toolbox" which is a software tool developed within the European MARS Crop Yield Forecasting System (Velde et al., 2019). The tool is designed specifically for this kind of analysis (Kerdiles et al. (2017), Goedhart et al. (2019)) and facilitates data storage, data analysis, time trend analysis of yield statistics, and performing (multiple) linear regression between reported yields and predictors. Moreover, the tool can work in an automated fashion enabling the analysis of a large number of regions as was necessary for this study.

## 4. Results

The four maps as described before are generated for all the crops and all three countries USA, India, and China. However, in this section, we will illustrate one example of each country that provides insight into the performance of the AgDMP product and uncertainties that arise from this analysis. Further, the results for the remaining maps of the crops for the three countries can be found in the supplementary material.

### 3.1. Maps depicting model skill

The maps shown in Fig. 6 show the % error reduction of TWSO and TAGP indicators relative to the baseline model. Regions are colored according to the percentage error reduction mentioned in the legend, dark blue denotes high skill with RMSE based on the AgDMP indicator more than 25% lower compared to the baseline, yellow indicates low to moderate skill (RMSE between 0 and 10% lower than the baseline) while orange and red colors indicate regions where the agDMP indicators have no skill (RMSE is higher than the baseline).

Fig. 6 illustrates that consistent high skill in both the indicators was observed for regions in the north-west, north-east, central-west, and south-east. Some regions in the central-east, eastern parts, and northern-south show inconsistent skill (showing skill in either one of the indicators).

In parts of central and eastern regions, the TAGP indicator showed high skill compared to the indicator TWSO. The north-eastern part (for example, Michigan state) showed that the TWSO indicator performed well compared to TAGP relative to the baseline predictor. However, in some parts of central and eastern regions and especially in western parts of the USA, there are regions with no skill for both the indicators (TWSO, TAGP). However, overall, the models including the TAGP indicator demonstrate skill for most regions for soybean in the USA.

Fig. 7 illustrates that high skill was observed for both the AgDMP indicators in many regions of China, particularly, for the major maize cropping zone which covers Heilongjiang, Jilin, and Inner Mongolia in the north-east, the North China plain, Shanxi and Shaanxi in the Central part of China, and Sichuan and Yunnan in the south. However, in the south-eastern part, there are regions with mixed results showing no skill for indicator TWSO. This particularly applies to the provinces of Hubei, Anhui, and Jiangsu. Skill in the western part of China is generally low but these are regions with low maize production and therefore of limited importance. Overall, both the indicators TAGP and TWSO demonstrate high skill in explaining yield variability for maize in China for the

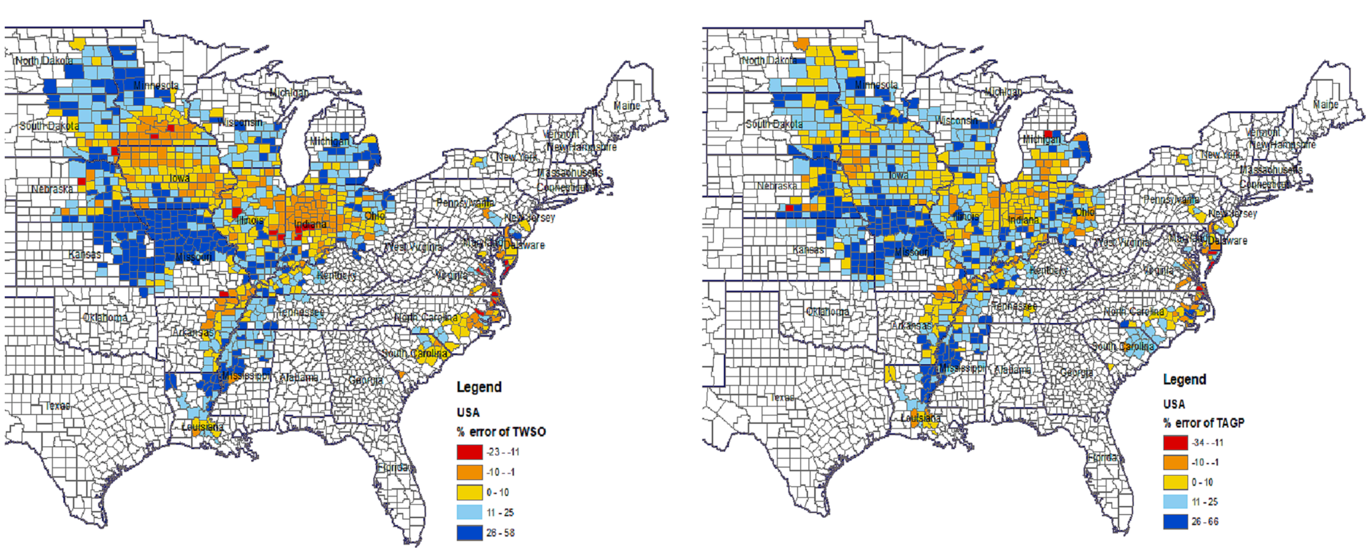


**Fig. 6.** Error of the prediction models using the AgDMP indicators TWSO (left) and TAGP (right) for soybean in the USA, expressed as a percentage of the error of the baseline predictor. Yellow to blue colours indicate regions where the model has a skill (reduced error compared to the baseline).

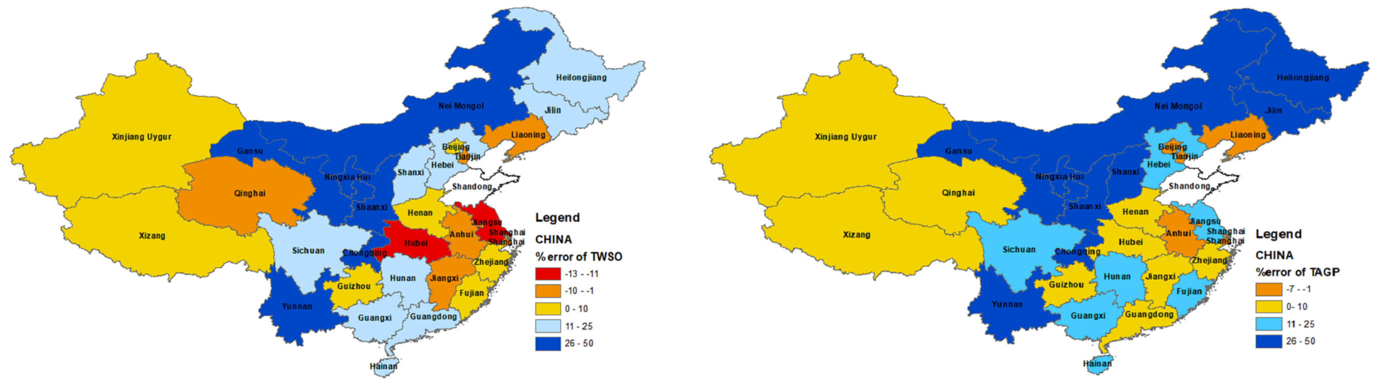


**Fig. 7.** Error of the prediction models using the AgDMP indicators TWSO (left) and TAGP (right) for maize in China, expressed as a percentage of the error of the baseline predictor. Yellow to blue colours indicate regions where the model has a skill (reduced error compared to the baseline).

important production areas. Except, in south-eastern China, where the TWSO does not perform well.

Fig. 8 shows the AgDMP skill for explaining the variability in rice yields in India. The results illustrate that both AgDMP indicators have skill in the regions in the southern part (Maharashtra, Karnataka, Tamil Nadu), the north-eastern part (Bihar, Assam, West-Bengal, Odisha) and in Punjab which are important rice production zones. Surprisingly, model skill is low (TAGP) or negative (TWSO) for Uttar Pradesh which is one of the major rice production zones in India. Overall, the AgDMP indicators have reasonable skill in explaining rice yield variability for the major production regions, except for Uttar Pradesh. The lack of skill in that region warrants a more detailed analysis which is beyond the scope of this study.

### *3.2. Map depicting the coefficient of determination*

Fig. 9 shows the coefficient of determination ($R^2$) between the indicators and the reported yield. Red implies no statistical significance, green implies correlation levels significant at 5% level, and blue at 1%. For most soybean production districts in the USA, a good correlation is obtained with a value ranging from 0.58 to 0.85. However, some districts, particularly in Iowa and Indiana, show no significant correlation between the TWSO and reported yields. To a lesser extent, this is also reflected in the coefficient of determination with the TAGP indicator but not as prominent. The districts along the eastern US coast show a mixed pattern of districts with poor correlation as well as high correlation. In general, the results from the correlation analysis are very similar to the results presented in Fig. 6. Districts with high coefficient of determination demonstrate high skill and vice-versa.

Fig. 10 illustrates the correlation between the AgDMP indicators and the reported yield of maize in China. The map demonstrates that the regions across the major maize production zone (Heilongjiang in the northeast, across central China to Yunnan in the southern part) have generally high coefficients of determination. Low coefficients of determination are present in the western part of China but these are regions with low maize-cultivated acreage. Finally, regions with low coefficients of determination can be found in the south-eastern part, particularly the provinces of Hubei, Hunan, Anhui, and Jianxi. In general, the regions which show no significant correlation between the indicators with the reported yields are the regions with low skill in both the indicators.

Fig. 11 shows the correlation between the indicators and reported yields for rice in India. The results show a significant correlation between the indicators and reported yield with a correlation value of 0.58–0.91 in some parts of the north-central, north-east, south-west, and

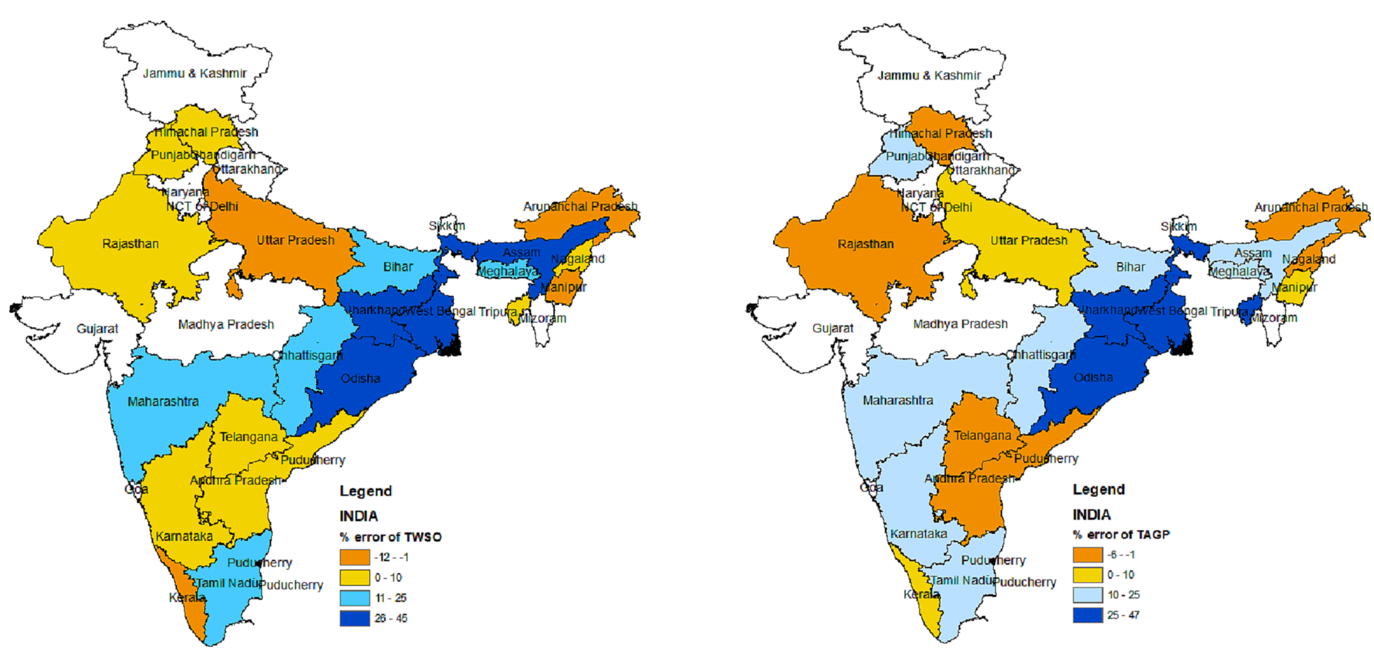


**Fig. 8.** Error of the prediction models using the AgDMP indicators TWSO (left) and TAGP (right) for rice in India, expressed as a percentage of the error of the baseline predictor. Yellow to blue colours indicate regions where the model has a skill (reduced error compared to the baseline).

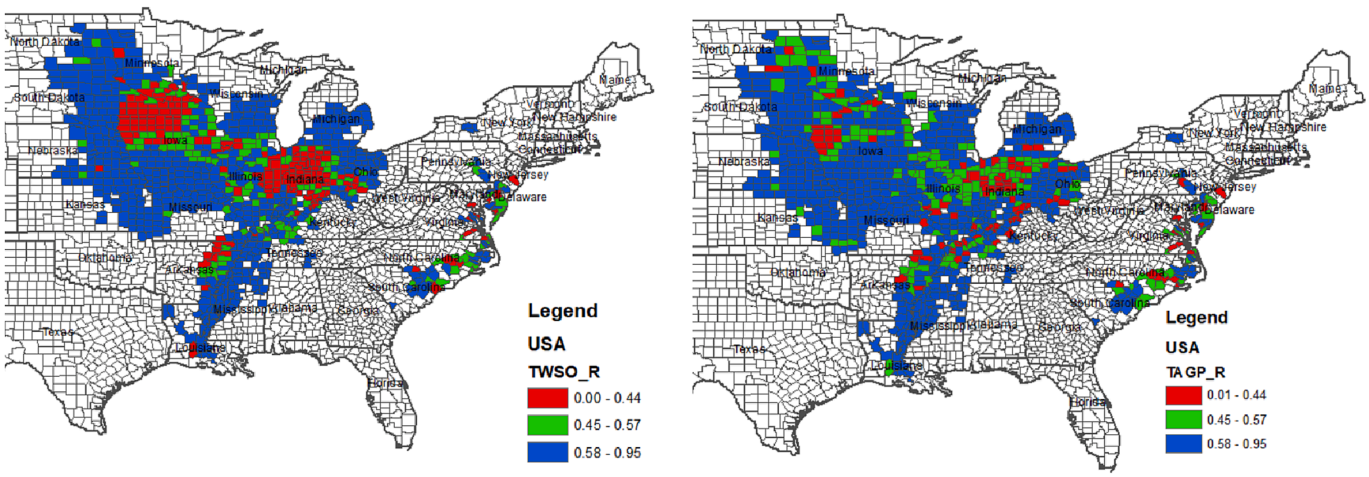


**Fig. 9.** Maps demonstrating the coefficient of determination ($R^2$) between the regional reported yield and the TWSO (left) and TAGP (right) indicators for soybean in the USA. Red implies no statistical significance, green implies correlation levels significant at 5% level, and blue at 1%.

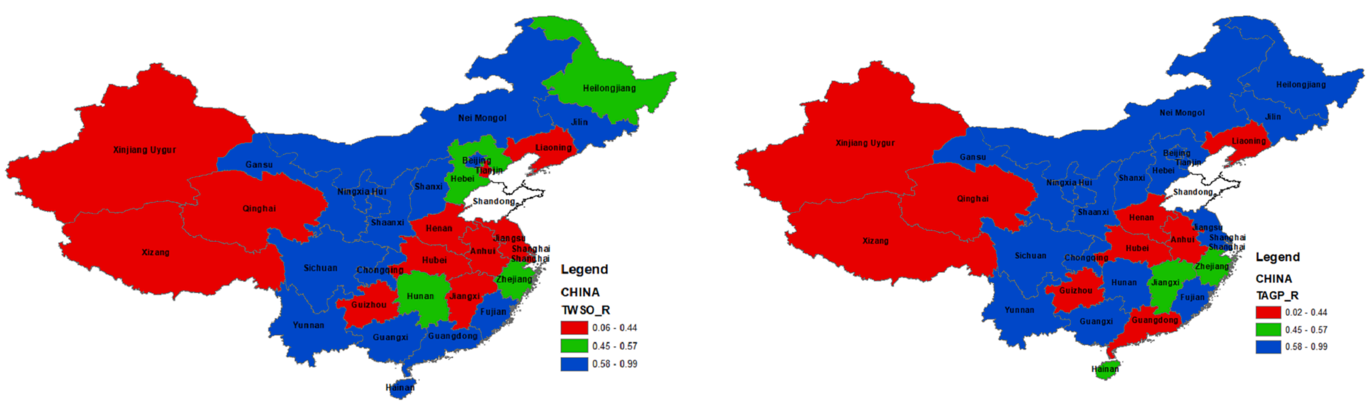


**Fig. 10.** Maps demonstrating the coefficient of determination ($R^2$) between the regional reported yield and the TWSO (left) and TAGP (right) indicators for maize in China. Red implies no statistical significance, green implies correlation levels significant at 5% level, and blue at 1%.

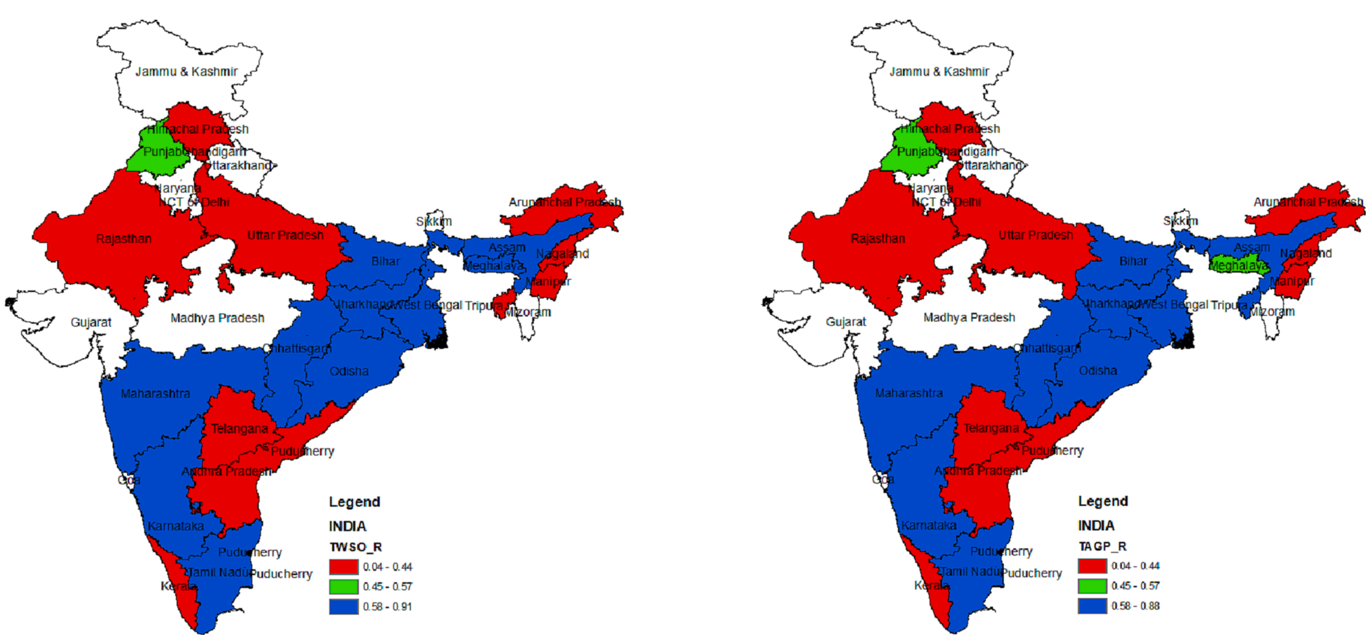


**Fig. 11.** Maps demonstrating the coefficient of determination ($R^2$) between the regional reported yield and the TWSO (left) and TAGP (right) indicators for rice in India. Red implies no statistical significance, green implies correlation levels significant at 5% level, and blue at 1%.

south-east. However, some of the regions in the south-east, north-west, and northeast show no significant correlation between the indicators TWSO and TAGP and the reported yields, whereas some regions in the northern and eastern parts of India show a significant correlation to the reported yields. Overall, both the indicators TWSO and TAGP perform similarly for rice crops in India.

### 3.3. Summarizing the results

The results were summarized per country and per crop type by counting in how many regions the TWSO and TAGP indicators outperformed the baseline predictor by 10–25% or by more than 25% (Table 1).

For rice in India in 5 out of 21 states, TWSO reduced the error skill by 10–25% and in a further 4 states, it did so by more than 25%. Together these 9 states represent 35.9% of India's total annual rice production. The counts in columns 2 and 4 may include different states (even when the administrative region (N) is identical), which is the reason that also columns 3 and 5 can differ. With a threshold of 10–25%, the indicator TAGP performed well for rice in India, while the indicator TWSO performed well for maize and wheat compared to TAGP. With greater than 25% error skill improvement, TAGP and TWSO performed almost the same in predicting rice and wheat crop yields. There is no improvement in error skills in soybean crops in India.

In the USA, TAGP performed well in predicting soybean and maize yields, compared to TWSO. However, in China TWSO performed well in the maize crop at 10–25%, while for the wheat crop at greater than 25%, compared to the performance of TAGP.

From Table 1, we can derive the indicator performance per crop type in three countries. It also shows the importance of the regions in terms of crop production by comparing the observed production percentages of regions showing improved error skills. Here, the production percentages are calculated using the reported statistics. However, in the table, for instance, TAGP performs best in China for rice and maize. The results indicate that both indicators performed well in many important producing areas of the USA, India, and China. However, if we compare both the indicator performance in terms of production totals in the USA, India, and China, TAGP contributes ~27–50% of total crop production in the USA and India and ~47–75% in China. While TWSO contributes ~24–41% in the USA and India, and 5–65% in China.

## 4. Discussion and conclusion

The overall conclusion is that the AgDMP indicators TWSO and TAGP show moderate to high skill in explaining the interannual yield variability in many important crop production regions in the USA, China, and India. The results demonstrate that the indicator TAGP usually has the highest skill as was shown for soybean and maize crops in the USA, for rice, maize, soybean, and wheat crops in China, and for rice, wheat, and maize crops in India. The TWSO indicator often has less skill and also shows more variability in skill.

However, there are also regions where both indicators have no skill. Often these are regions with limited importance due to a low crop acreage but in some cases, this also occurs in major production areas. For example, in certain districts of the US corn belt (mainly in Iowa, Indiana, and Illinois – see Fig. 6 and Fig. 9) both TAGP and TWSO do not show any skill. Such areas will require additional analysis to explain the lack of skill. A possible cause could be related to the cropping pattern followed in the corn belt region which is continuous maize and alternating maize and soybean two-year rotation. Therefore the poor skill could be due to not properly accounting for the shift in the development of the crop in the cropping calendar.

Although the overall results are quite satisfactory, there are also some clear limitations of the current implementation of AgDMP. First of all, the AgDMP processing chain does not include a water balance. Instead, the water limitations are expressed through reduced canopy

**Table 1**
A number of administrative regions (N) in all three countries where the RMSE of TWSO and TAGP indicators is smaller than the baseline predictor by 10–25% or by more than 25%. Also shown are the contributions (%) that the improved regions make to the country's total production.

| Crop | TWSO N | Production % | TAGP N | Production % | Total Administrative regions | TWSO N | Production % | TAGP N | Production % | Total Administrative regions | TWSO N | Production % | TAGP N | Production % | Total Administrative regions |
|---|---|---|---|---|---|---|---|---|---|---|---|---|---|---|---|
| 1 | 2 | 3 | 4 | 5 | 6 | 2 | 3 | 4 | 5 | 6 | 2 | 3 | 4 | 5 | 6 |
| India | | | | | states | USA | | | | counties | China | | | | provinces |
| 10-25% improvement | | | | | | | | | | | | | | | |
| Rice | 5 | 20.1 | 7 | 29.4 | 21 | - | - | - | - | - | 3 | 12.0 | 10 | 46.4 | 25 |
| Maize | 3 | 16.6 | 2 | 12.4 | 21 | 221 | 14.3 | 319 | 23.01 | 1076 | 9 | 48.6 | 6 | 21.5 | 30 |
| Wheat | 5 | 34 | 3 | 20.0 | 14 | - | - | - | - | - | 6 | 12.4 | 6 | 54.6 | 22 |
| Soybean | - | - | - | - | 8 | 286 | 23.5 | 344 | 27.7 | 927 | 2 | 3.8 | 5 | 11.6 | 24 |
| >25% improvement | | | | | | | | | | | | | | | |
| Rice | 4 | 15.8 | 4 | 17.7 | 21 | - | - | - | - | - | 1 | 0.8 | 2 | 1.3 | 25 |
| Maize | 1 | 7.6 | 4 | 17.1 | 21 | 149 | 9.6 | 389 | 27.3 | 1076 | 6 | 16.5 | 9 | 53.3 | 30 |
| Wheat | 1 | 7.4 | 1 | 7.4 | 14 | - | - | - | - | - | 5 | 36.1 | 3 | 5.2 | 22 |
| Soybean | - | - | - | - | 8 | 233 | 17.7 | 222 | 17.3 | 927 | 1 | 2.0 | - | - | 24 |

light interception from a reduction in the satellite observed FAPAR. This means that only when there is such a shortage of water that the leaves are dying it can be observed by the satellite. Thus, only long-term drought effects are reflected in the product data, whereas short-term drought effects cannot be accounted for properly. However, mild water shortages during vegetative/crop growth reduce plant height and decrease the dry biomass and yield (Cakir, 2004). In China and India, both rainfed and irrigated farming systems occur. Uneven distribution of rainfall and irrigation water may lead to a shortage of water and will increase the yield variation. This variation of the yield parameters such as plant height, biomass, and yield may also lead to poor relations between the indicators with reported yields. In general, the observed poor performance in some regions may be due to not properly accounting for the impact of short-term droughts.

Second, the satellite-derived FAPAR data used as input for AgDMP have a spatial resolution of 1 km and are aggregated based on a crop dominance mask with a resolution of 1 km. This generally means that only areas with cropping patterns consisting of a few dominant crops are included in the AgDMP product. For instance, areas with smallholder farming are excluded because the cropping pattern cannot be resolved at 1 km resolution. Consequently, the indicators are not useful for the analysis of crop productivity in regions with smallholder agriculture. Areas with the lowest crop production showed a quite poor relation. In India, both indicators do not explain the variability of soybean yield well. This is because soybean is rarely the dominant crop and therefore is not well represented in the fAPAR measurements.

Third, the crop dominance mask is a static product, while cropping areas may change or expand, and thus this crop dominance mask may have limited accuracy. These problems mostly occur in complex terrain regions and with mosaics landscapes of mixed natural vegetation and agriculture (Liu et al., 2020). For example, in such cases that satellite pixels with thick and evergreen forests can be misclassified as rice, which leads to unrealistic results in simulation. In China, the poor performance observed in the north-eastern part and western parts probably results in a form that has a complex terrain and mix of agriculture and forestry. Similarly, in India, the northern part is covered with forest which may lead to uncertainties in the result.

Finally, the crop calendars used in the AgDMP product are derived from the Global Agro-Ecological Zonation (Fischer et al. 2021) or the SAGE crop calendars (Sacks et al. 2010). Both datasets have limitations that may lead to a shifted crop calendar compared to the local cropping calendar. This will have a direct impact on the quality of the AgDMP product because the crop model will be poorly aligned with the FAPAR time series. An update of the AgDMP product should therefore focus on improving the cropping calendars, possibly deriving them from the satellite time series directly (Kotsuki and Tanaka, 2015).

Despite the limitation discussed above, our results demonstrate that the AgDMP product has considerable skill in explaining interannual yield variability and therefore is suitable for analyzing crop productivity at a regional scale. Moreover, the near-real-time availability of AgDMP means that the product can be used for analyzing the crop status of the current cropping season. Although the precocity of the AgDMP product has not been analyzed (we only analyzed end-of-season results), this paves the way for the possible use of AgDMP for yield prediction which would be valuable for policy decisions, market analysis, and commodity trading.

## CRediT authorship contribution statement

**Sneha Chevuru:** Writing – original draft, Conceptualization, Formal analysis, Validation. **Allard de Wit:** Supervision, Conceptualization, Resources, Writing – review & editing. **Iwan Supit:** Writing – review & editing. **Ronald Hutjes:** Supervision, Conceptualization, Writing – review & editing.

## Declaration of Competing Interest

The authors declare that they have no known competing financial interests or personal relationships that could have appeared to influence the work reported in this paper.

## Data availability

I have shared the link to my data

## Acknowledgment

This paper builds on results from the Copernicus C3S_422_Lot1_-WEnR – Global Agriculture contracts led by Wageningen Environmental Research (WENR), which focused on the development of crop productivity indicators within the context of the Copernicus Climate Change Service (C3S) implemented by the European Centre for Medium-Range Weather Forecasts (ECMWF) and funded by the European Union.

## Appendix A. Supplementary data

Supplementary data to this article can be found online at https://doi.org/10.1016/j.cliser.2023.100374.

## References

Adiele, J.G., Schut, A.G.T., van den Beuken, R.P.M., Ezui, K.S., Pypers, P., Ano, A.O., Egesi, C.N., Giller, K.E., 2021. A recalibrated and tested LINTUL-Cassava simulation model provides insight into the high yield potential of cassava under rainfed conditions. Eur. J. Agron. 124, 126242 https://doi.org/10.1016/j.eja.2021.126242.

Arata, Linda, Enrico Fabrizi, and Paolo Sckokai. "A Worldwide Analysis of Trend in Crop Yields and Yield Variability: Evidence from FAO Data." Economic Modelling 90 (August 1, 2020): 190–208. 10.1016/j.econmod.2020.05.006.

Becker-Reshef, I., Barker, B., Humber, M., Puricelli, E., Sanchez, A., Sahajpal, R., Prakash, A., 2019. The GEOGLAM crop monitor for AMIS: Assessing crop conditions in the context of global markets. Glob. Food Sec. 23, 173–181.

Becker-Reshef, I., Justice, C., Whitcraft, A. K., & Jarvis, I. (2018, July). Geoglam: A Geo Initiative on Global Agricultural Monitoring. In IGARSS 2018-2018 IEEE International Geoscience and Remote Sensing Symposium (pp. 8155-8157). IEEE.

Buontempo, C., Hutjes, R., Beavis, P., Berckmans, J., Cagnazzo, C., Vamborg, F., Ramasamy, S., 2019. Fostering the development of climate services through Copernicus Climate Change Service (C3S) for agriculture applications. Weather and Climate Extremes, 100226.

Cakir, R., 2004. Effect of water stress at different development stages on vegetative and reproductive growth of corn. Field Crop Res 89 (1), 1–16.

Connor, D.J., Loomis, R.S., Cassman, K.G., 2011. Crop Ecology. Productivity and Management in Agricultural Systems. Cambridge Univ. Press, Cambridge, UK.

De Wit, A., Hutjes, R., 2019. Product User Guide and Specification data stream 3: Copernicus climate enhanced, EO-based crop productivity and evapotranspiration products. https://sis-dev.climate.copernicus.eu/cdsapp#!/dataset/sis-crop-productivity-indicators?tab=doc accessed by 12/03/2020.

De Wit, A., Boogaard, H., Fumagalli, D., Janssen, S., Knapen, R., van Kraalingen, D., van Diepen, K., 2019. 25 years of the WOFOST cropping systems model. Agr. Syst. 168, 154–167.

FAOSTAT, 2014. Asia and Pacific agriculture.

Fischer, G., Nachtergaele, F. O., van Velthuizen, H., Chiozza, F., Francheschini, G., Henry, M., ... & Tramberend, S. (2021). Global Agro-ecological Zones (GAEZ v4)-Model Documentation.

Foley, J.A., Ramankutty, N., Brauman, K.A., Cassidy, E.S., Gerber, J.S., Johnston, M., Mueller, N.D., O/'Connell, C., Ray, D.K., West, P.C., Balzer, C., Bennett, E.M., Carpenter, S.R., Hill, J., Monfreda, C., Polasky, S., Rockstrom, J., Sheehan, J., Siebert, S., Tilman, D., Zaks, D.P.M., 2011. Solutions for a cultivated planet. Nature 478, 337-342.

Gadde, B., Bonnet, S., Menke, C., Garivait, S., 2009. Air pollutant emissions from rice straw open field burning in India, Thailand and the Philippines. Environ.Pollut. 157 (5), 1554–1558.

Gao, X., Cheng, W., Wang, N., Liu, Q., Ma, T., Chen, Y., Zhou, C., 2019. Spatio-Temporal Distribution and Transformation of Cropland in Geomorphologic Regions of China during 1990–2015. J. Geog. Sci. 29 (2), 180–196. https://doi.org/10.1007/s11442-019-1591-4.

Goedhart, Paul, Steven Hoek, and Hendrik Boogaard. "The CGMS Statistical Tool User Manual v 3.5.3." Luxembourg: European Commission, 2019. https://mars.jrc.ec.europa.eu/asap/files/CGMS-Statistical-Tool-V_3_5_3.pdf.

Grassini, P., Specht, J.E., Tollenaar, M., Ciampitti, I., Cassman, K.G., 2014. High-yield maize–soybean cropping systems in the US Corn Belt. In: Sadras, V.O., Calderini, D.F. (Eds.), Crop Physiology, 2nd ed. Academic Press, San Diego.

Kearney, J., 2010. Food consumption trends and drivers. Philos. Trans. R. Soc. London B: Biol. Sci. 365, 2793–2807.

Kerdiles, H., F. Rembold, O. Leo, H. Boogaard, and S. Hoek. "CST, a Freeware for Predicting Crop Yield from Remote Sensing or Crop Model Indicators: Illustration with RSA and Ethiopia." In 2017 6th International Conference on Agro-Geoinformatics, 1–6, 2017. 10.1109/Agro-Geoinformatics.2017.8047071.
Kotsuki, S., Tanaka, K., 2015. SACRA–a method for the estimation of global high-resolution crop calendars from a satellite-sensed NDVI. Hydrol. Earth Syst. Sci. 19 (11), 4441–4461.
Krishisewa, 2013. Maize and Soybean: The Potential Crops for Agricultural Growth. https://www.krishisewa.com/articles/production-technology/260-maize-soybean-cultivation.html.
Liu, X., Zhai, H., Shen, Y., Lou, B., Jiang, C., Li, T., Shen, G., 2020. Large-scale crop mapping from multisource remote sensing images in Google Earth Engine. IEEE J. Sel. Top. Appl. Earth Obs. Remote Sens. 13, 414–427.
Livezey, J., Foreman, L., 2004. Characteristics and production costs of U.S. rice farms. US Dept. of Ag. Statistical Bulletin. 974-7.
Muthayya, S., Sugimoto, J.D., Montgomery, S., Maberly, G.F., 2014. An overview of global rice production, supply, trade, and consumption. Ann. N. Y. Acad. Sci. 1324 (1), 7–14.
Sacks, W.J., Deryng, D., Foley, J.A., Ramankutty, N., 2010. Crop planting dates: an analysis of global patterns. Glob. Ecol. Biogeogr. 19 (5), 607–620.
Smith, L. E. D., Siciliano, G., "A Comprehensive Review of Constraints to Improved Management of Fertilizers in China and Mitigation of Diffuse Water Pollution from Agriculture." Agriculture, Ecosystems & Environment, Sustainable intensification of China's agriculture: the key role of nutrient management and climate change mitigation and adaptation, 209 (November 1, 2015): 15–25. 10.1016/j.agee.2015.02.016.
Smith, W.K., Fox, A.M., MacBean, N., Moore, D.J.P., Parazoo, N.C., 2020. Constraining estimates of terrestrial carbon uptake: new opportunities using long-term satellite observations and data assimilation. New Phytol. 225 (1), 105–112. https://doi.org/10.1111/nph.16055.
Sugg, Z., 2007. Assessing U.S. farm drainage: can GIS lead to better estimates of subsurface drainage extent? World Resources Institute, Washington D.C [online WWW]. Available URL:http://pdf.wri.org/assessing_farm_drainage.pdf.
Thenkabail, Prasad, Knox, Jerry, Ozdogan, Mutlu, Gumma, Murali, Congalton, Russell, Wu, Zhuoting, Milesi, Cristina, et al. "NASA Making Earth System Data Records for Use in Research Environments (MEaSUREs) Global Food Security Support Analysis Data (GFSAD) Crop Dominance 2010 Global 1 Km V001." NASA EOSDIS Land Processes DAAC, 2016. 10.5067/MEASURES/GFSAD/GFSAD1KCD.001.
van der Velde, M., van Diepen, C.A., Baruth, B., 2019. The European crop monitoring and yield forecasting system: celebrating 25 years of JRC MARS bulletins. Agr. Syst. 168, 56–57. https://doi.org/10.1016/j.agsy.2018.10.003.